

# STEPS FOR CONDUCTING A VALID HYDRAULIC-FRACTURING LABORATORY TEST



Lead Author  
Mohammad  
Sarmadivaleh

**M. Sarmadivaleh, B. Joodi, A. Nabipour and V. Rasouli**  
Department of Petroleum Engineering  
Curtin University  
26 Dick Perry Avenue  
Kensington WA 6151  
mohammad.sarmadivaleh@curtin.edu.au

## ABSTRACT

Several parameters are involved in a hydraulic-fracturing operation, which is a technique used mainly in tight formations to enhance productivity. Formation properties, state of stresses in the field, injecting fluid characteristics, and pumping rate are among several parameters that can influence the process. Numerical analysis is conventionally run to simulate the hydraulic-fracturing process. Before operating the expensive fracturing job in the field, however, it would be useful to understand the effect of various parameters by conducting physical experiments in the lab. Laboratory experiments are also valuable for validating the numerical simulations. Applying the scaling laws, which are to correspond to the field operation with the test performed in the lab, are necessary to draw valid conclusions from the experiments. Dimensionless parameters are introduced through the scaling laws that are used to scale-down different parameters including the hole size, pump rate and fluid viscosity to that of the lab scale. Sample preparation and following a consistent and correct test procedure in the lab, however, are two other important factors that play a substantial role in obtaining valid results. The focus of this peer-reviewed paper is to address the latter aspect; however, a review of different scaling laws proposed and used will be given.

The results presented in this study are the lab tests conducted using a true triaxial stress cell (TTSC), which allows simulation of hydraulic-fracturing under true field stress conditions where three independent stresses are applied to a cubic rock sample.

## KEYWORDS

Hydraulic-fracturing, laboratory test, scaling laws, sample preparation, triaxial stress cell.

## TEST EQUIPMENT AND SAMPLE PREPARATION

A proper hydraulic-fracturing experiment is one that is conducted under true field stress condition; That is, three stresses are applied to the sample independently. Practically, this is not applicable unless the sample is of cubic shape, contrary to cylindrical samples that are tested in rock mechanics labs. In this case, the stresses are applied to the sample faces using hydraulic rams or a flat jack. The use of rectangular shaped samples—used by some people (e.g., Rabaa, 1987)—adds more complexity to the design of the test and provides more length along the longer side of the sample for the fracture to propagate during the experiment. The simulation of underground stress in the

laboratory applies a tremendous amount of load that should be distributed uniformly on the sample. As an example, the vertical load that should be applied on a cubic sample of 20 cm (7.84 in) to simulate the effective stresses at a depth of 2,743 m (9,000 ft) will be  $1.395 \times 10^6$  N (313,659 lbf) considering the normal and overburden pressure gradient of 9.81 kPa/m (0.433 psi/ft) and 22.66 kPa/m (1.0 psi/ft), respectively. The friction generated between the rams and the sample face may cause a change in stress distribution on the sample (Vonk, 1993). This effect may be reduced by inserting a very thin Teflon sheet and applying grease as a lubricant. Failure to consider this effect may cause zonal stress intensity, which could disturb the fracture path. This may be considered as the main advantage of using a flat jack over hydraulic rams for applying the stress to the sample. The deficiencies associated with flat jacks, however—including their regular failure during operation, their needs for systematic calibration, and their efficiency—are factors that make the use of flat jacks more complicated for these types of applications. On the other hand, ultra-large-sized hydraulic rams are required to apply high stresses on large samples, which in turn require large and heavy supporting frames. The uniformity of distributed stresses on the sample should be examined in each test. This may be done by acoustic transmission (to check if sound velocity is similar in all cross sections) or by instrumenting the ram plates through which the stresses are applied to the sample. This could be implemented by mounting strain gauges on the plates that apply the stresses to the sample. Alternatively, strain gauges may be embedded inside the sample body or on its surface. Fracture pressure analysis during and after the fracturing test may be used for this purpose as well, especially by checking the closure pressure and fracture geometry to obtain an average normal stress acting on the fracture surface. Table 1 contains a summary of the specifications of some of the true triaxial lab equipment used for hydraulic-fracturing experiments around the world.

To conduct a lab experiment, the natural rock sample should be cut, trimmed and polished precisely. This makes the cost of the sample preparation expensive. Alternatively, artificial cement samples may be prepared by casting mortar, which is relatively cheap and reliable if the curing process is applied correctly. In the experiments performed for the purpose of this study, which used a true triaxial stress cell (TTSC), mortar samples were prepared. For this purpose, water, sand, and cement were mixed for 15 min. This time was found to be adequate to ensure the sand grain distribution was uniformly shaped in the mortar. The mix was poured into different mould sizes gradually while a vibration was used to remove the air bubbles trapped in the mix. The vibration time period was chosen in such a way that sand particles were not precipitating as mixture viscosity was relatively large to suspend them during the course of vibration. The top side of the sample was flattened using a finishing trowel one hour after casting. This is because the mix will release some bleed water and, consequently, shrink slightly. The sample was then removed carefully from the mould after 12 hours and cured for 28 days in 25°C water bath.

It is expected that the cement cubes obtain their final strength (i.e., more than 90%) after 28 days (Mindess et al, 2003). For mortar with no or low amount of sand, retarders like sodium chloride (NaCl), with less than 5 wt%, may be used to decelerate the exothermic cement hydration process. This prevents fast dehydration of the mortar, therefore avoiding generation of micro cracks. At micro scale these blocks may have small pore spaces of 1  $\mu\text{m}$ , enclosed with grains of 11, 000  $\mu\text{m}$  size (de Ketterij, 2001). The low fracture toughness, low permeability, and low to moderate porosity are the key features that make the cement a good candidate for fracturing tests. A minimum of three cylindrical samples of 38 $\times$ 76 mm (1.5 $\times$ 3 in diameter  $\times$  length) should be made for each sample to conduct standard hydro-mechanical tests. These samples were used for permeability, porosity, uniaxial compressive strength (UCS), confined compressive strength, and multi stage compressive tests. Also, a few larger-diameter cylindrical samples were used for Brazilian and fracture toughness tests. For the sake of simplicity, tensile strength and fracture toughness values can be estimated indirectly from Brazilian and mode I Semi-Circular Bend (SCB) tests, respectively (Chong et al, 1987). These same tests should be done several times to make sure that the final results are a good representation of the average hydro-mechanical properties prepared by mortar. These results provide enough information for the scaling analysis procedure. Table 2 summarises the hydro-mechanical properties of the samples and the method used to measure each property for one mortar sample prepared for a series of fracturing tests.

## HYDRAULIC-FRACTURING

As drilling a dried sample may create small cracks around the wellbore, the samples were drilled through immediately after they were removed from the water bath. A very slow drilling speed should be used and different drill bits with different lengths should be attempted to ensure the hole is drilled with minimum

damage to the sample. Alternatively, the hole (plus the notch to help with the initiation of a fracture plane around the borehole) may be made during the casting process of the samples.

The hole was drilled through the entire sample length to ensure no new stress disturbances were introduced to the rock due to partial penetration. A quarter-inch tubing size was used as the injection line for fracturing fluid. A couple of axial notches (in case of vertical fracture) or a round circumferential groove (in case of horizontal fracture), were made along the mid length of the inside wall of the wellbore to promote the fracture initiation. This was made using a small turning bend. The depth of notches was a few millimetres. It is understood that the best practice is to apply the maximum stress during the test perpendicular to the direction of the notches for easy fracture initiation. If this is not the case, the fracture may initiate in a direction different than the maximum stress direction, but then reorient to align itself to this direction after propagating some distance away from the wellbore. The fracture initiation would be very difficult without having the notches on a homogeneous and smooth borehole wall.

There is a threshold for notch depth to provide stress concentration for a horizontal fracture to initiate correctly (Lhomme, 2005). To explain the importance of having a proper notch for fracture initiation, an example of a fracture test is explained here. Figure 1 shows the sample view after a fracturing test on a 20 cm block. The test was designed for horizontal fracture propagation and the sample was equipped with six pressure monitoring probes aiming to detect fracture arrival at different distances away from the wellbore wall. In absence of a proper horizontal notch, however, the fracture initiated in a vertical plane, and some distance away from the wellbore, it changed its orientation into a horizontal plane. The results of some other experiments the authors performed indicated that without using notches, fracture initiation may occur at multiple points. In the example explained here, a twisted fracture plane was produced, which is not favourable.

**Table 1.** Some of the past equipment used for hydraulic fracturing lab experiments (Sarmadivaleh, 2012). HR: hydraulic ram; FJ: Flat Jack; ST: screw type.

	Sample dimension	Vertical stress $\sigma_v$	Min. horizontal stress $\sigma_{nMin}$	Max. horizontal stress $\sigma_{HMa}$	Cell fluid pressure $P_f$	Injection pressure $P_{inj}$
TerraTek	27 $\times$ 27 $\times$ 32 in (69 $\times$ 69 $\times$ 81 cm)	FJ 8,000 psi (55 MPa) or HR 1.7 $\times$ 106 lbf	FJ 8,000 psi (55MPa)	FJ 8,000 psi (55MPa)	Yes >2,000psi	N/A
	11 $\times$ 11 $\times$ 15 in	FJ 4,500 psi	FJ 4,500 psi	FJ 4,500 psi	N/A	N/A
Delft University	12 $\times$ 12 $\times$ 12 in (30 $\times$ 30 $\times$ 30 cm)	HR 5,700 psi (38.9 MPa)	HR 5,700 psi 38.9 MPa	HR 5,700 psi 38.9 MPa	No	50M Pa 0.1–100 cc/min 300 cc
Haliburton	5 $\times$ 5 $\times$ 5.5 in	HR 0.1 $\times$ 106 lbf	FJ 2,500 psi	FJ 2,500 psi	N/A	4–600 psi/s
	6 $\times$ 12 $\times$ 18 in	ST 0.12 $\times$ 106 lbf	HR 3,000 psi	HR 3,000 psi	N/A	10,000 psi, 500 cc/min
University of Oklahoma	18.75 $\times$ 18.75 $\times$ 18 in	FJ 3,000 psi	FJ 3,000 psi	FJ 3,000 psi	No	10,000 psi, 1.4 cc/min
Eindhoven University of Technology	20 $\times$ 10 $\times$ 10 cm	HR 0.4 $\times$ 106 lbf	HR 0.4 $\times$ 106 lbf	HR 0.4 $\times$ 106 lbf	No	N/A
CSIRO*	40 $\times$ 40 $\times$ 40 cm	FJ 25 MPa	FJ 25 MPa	FJ 25 MPa	No	70 MPa
Petroleum University of China	12 $\times$ 12 $\times$ 12 in	FJ 5,700 psi	FJ 5,700 psi	FJ 5,700 psi	No	20,300 psi

\*Smaller set of flat jacks may be used to apply a higher stress to smaller samples.

The open hole section is isolated between the metal bar, inserted to act as casing on top, and the injection tube at the bottom. Both the casing and tube must be nicely glued to make a proper isolation of the open hole section for hydraulic-fracturing purposes. Also, special care should be taken for drying the wellbore wall to ensure the glue forms a firm bond between the rock and metals. Figure 2 shows the sample with a drilled hole in the centre. This figure also illustrates the glued top casing and bottom injection tube, as well as the vertical notches in the middle of the drilled hole.

The stresses are applied in steps. First the authors increased all three stresses simultaneously to the minimum in-situ stress magnitude. One stress is then kept constant along the chosen direction for minimum stress; this is done using a constant pressure schedule in the syringe pump controller for that stress. The other two stresses are increased to the magnitude of the intermediate stress. This intermediate stress is then kept constant, now simulating the intermediate stress along the preferred direction, and the third stress is increased to the desired value. The injection tube is now connected to the injection system and the data acquisition system records all data during the course of fluid injection.

The use of a flow restriction device before the last transducer would help immensely to gradually regulate the flow of a large

volume of fracturing fluid into a newly initiated fracture plane. This large flow rate is driven by the compressibility of fracturing fluid plus hydraulic oil in the displacement chamber and, to a lesser extent, the volume change of the metal pressure vessels. The flow restriction device will reduce unstable fracture growth, especially during the fracture initiation. This can be done by using a choke (a slightly opened needle valve) located at the point of injection, preferably between two pressure transducers to record restricted and pump pressures in the flow line (Bunger, 2005).

## SCALING LAWS

To consider a hydraulic-fracture field test being simulated at laboratory scale, scaling laws are to be applied to the fracturing parameters. This is briefly discussed below; however, many experiments have been carried out without using scaling as part of the experimental design. Most of the hydraulic-fracturing tests performed in the laboratory represent a highly exaggerated injection rate and a very low fluid viscosity as they used a fracturing fluid very similar to what is being used in a real fracturing job in the field (Weijers, 1995). To monitor fracture propagation in a reasonable time on a sample that can be handled in the laboratory, however, a fluid with much higher

**Table 2.** The hydro-mechanical properties of the cement sample and the measurement method at which the measurements were arranged.

Hydro-mechanical property	Value	Test method
Uni-axial compressive strength, UCS psi (MPa)	11,530 ±750 (79.5)	Unconfined compression test
Uni-axial poisson's ratio, $\nu$	0.197± 0.02	Unconfined compression test
Young's modulus, E, psi (GPa)	4.018×106 ± 2×105 (27.74)	Unconfined compression test
Internal friction coefficient, $\Phi$ (degree)	44.3	Mohr circle, confined test
Cohesion, Cc psi (MPa)	2,524 (17.3)	Mohr circle, confined test
Tensile strength, T0, psi (MPa)	510±200 (3.5)	Brazilian tensile test
Fracture toughness, KIC, psi Öin (MPaÖm)	710±200 (0.78)	CSB
Porosity, f %	14.7±1	Boyle's law porosimeter
Permeability, K mD	0.018±0.005	Transient gas flood

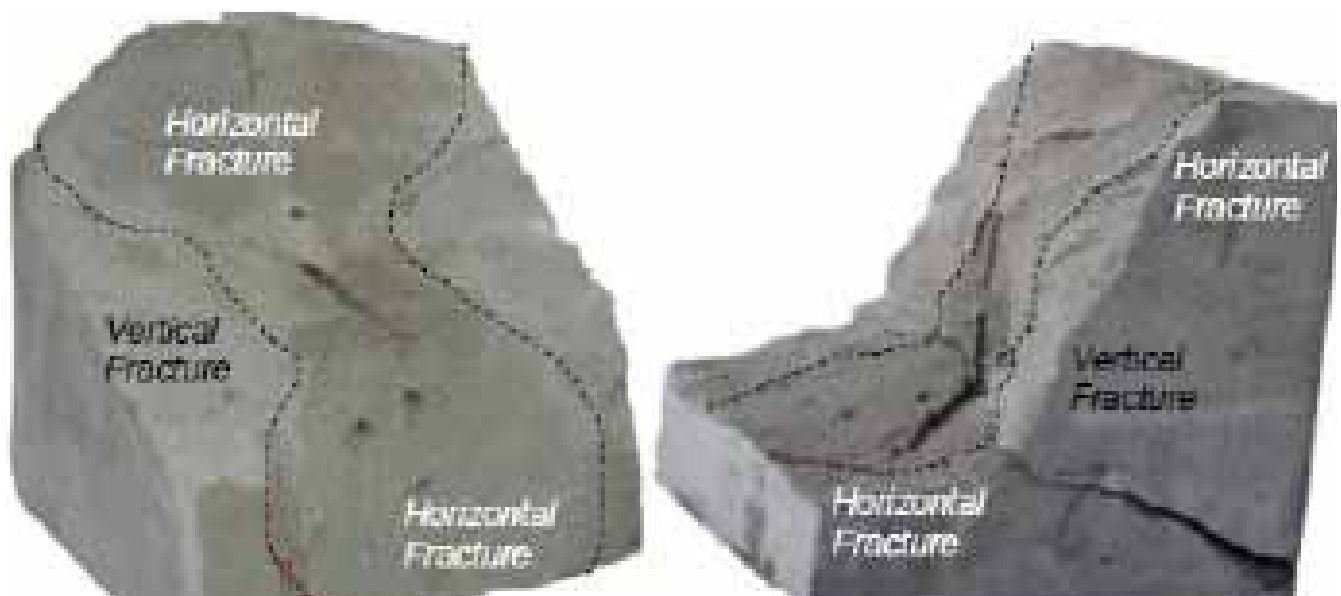


**Figure 1.** An example of twisted fractured plane caused by improper notch placement.

viscosity is typically required when using a low injection rate. This ensures that the hydraulic fracture is contained inside the sample boundaries and the propagation can be monitored without being affected by the boundary conditions.

The scaling laws are applied to model field representative fracture growth in the lab by defining the fracturing parameters (e.g., viscosity) in such a way that the laboratory and field fracture propagation regimes are as similar as possible (de Pater, 1994; Bunger et al, 2005). For a driven hydraulic fracture, the dominant factor that governs the energy and mass balance processes depends on the propagation regime; the scaling design is dependent on this factor (Adachi, 2001; Detournay, 2004). In a small-scale laboratory test considering the case of a penny-shaped fracture, it is most likely that toughness controls the fracture propagation regime at the final stage of propagation after a period of specific time; however, almost all of the field-scale hydraulic fractures over nearly all of their propagation history are viscosity dominated (Cleary, 1980; Detournay, 2004; Adachi et al, 2007). This means the main energy dissipation mechanism is viscosity, and the energy of the fracturing fluid was used to keep fluid moving in the fracture path and penetrate the newly generated surface.

For this purpose, dimensionless groups of physical parameters, describing a specific fracturing process, are defined in the way they become identical by using lab and field parameters. These dimensionless variables are driven from the fluid flow (mass and momentum conservation laws) and rock behaviour (rock deformation, crack opening, and extension) partial differential equations. As one simple approach, the results of such calculations could be represented in a parametric space with three extreme boundaries of viscosity, toughness, and leak-off dominated propagation regimes, as depicted in Figure 3 (Bunger, 2005). It is worth mentioning that in general, a parametric space with infinite edges (rather than three) could be assumed; however, one or a few of these parameters will govern the overall process at any specific time (Bunger, 2005). In this paper, this triangular parametric space will be used as part of the scaling analysis.

The importance of using the term, specific time, should be highlighted here because the dominant propagation regime may change from one time to another during a single fracturing test. The fracture propagation mechanism, hydro-mechanical properties of the rock, fluid properties, and flow rate at a specific time determine the propagation regime; that is, the location of the fracture evolution in the parametric space. Proposed scaling scenarios have been considered in literature that include cases with different combinations of zero, small,

finite, and large toughness for permeable or impermeable rocks that are being fractured using viscous or inviscid fluid (Adachi and Detournay, 2002; Savitski and Detournay, 2002; Bunger, 2005; Bunger et al, 2005b; Garagash and Detournay, 2005; Lhomme, 2005; Garagash, 2006; Adachi and Detournay, 2007; Mitchell et al., 2007).

While the scaling laws can be applied, the heterogeneous nature of the rock samples at the small size considered means the impact of micro heterogeneities on the fracture propagation pattern (e.g., pore size distribution and pore shape, and small beddings or facies) presents a difficulty for extrapolating the results to large scales. Scaling micro-structural properties like the ratio of the fracture length to grain size in lab or field operation is not practically a possible task (de Pater, 1994). Therefore, the effect of the grain size on fracture propagation is neglected in all studies, including the present work.

In real field fracturing operations, fracture extension toughness is dominated at the early stages of propagation, during initiation, but rapidly becomes viscous dominated (Mack and Warpinski, 2000). Finally, for a radial fracture, it again becomes toughness dominated (Detournay, 2004). The scaling laws proposed by de Pater et al (1994) can be used for determining the fracturing conditions, especially when synthetic mortar samples are being used for the laboratory test. The final laboratory conditions, however, must be checked against other more recent scaling studies (i.e., Detournay, 2004; Bunger, 2005; Lhomme, 2005). It is to be noted that a similar scaling approach has been used for laboratory fracturing tests for a few other rock types, but with different sample sizes (e.g., Athavale, 2008).

The fracture propagation period, or the scaled time of fracturing, starts at the initiation of the fracture. It then counts down until the final value that was calculated previously. The initiation time itself is defined as the moment the wellbore pressurisation rate reaches its maximum value. Fracture breakdown is usually defined as the time at which wellbore pressure reaches its maximum value (Lhomme, 2005); fracture initiation typically occurs before this breakdown point. The scaling period is valid from initiation until stopping the injection of fluid. For viscose dominated fracture propagation, equation 1 should be met during fracture propagation (de Pater, 1994).

$$K_{ic} < 2P_n \sqrt{\frac{r_f}{\pi}} \tag{1}$$

In Equation 1,  $r_f$  is fracture radius and  $P_n$  is fracture net pressure. For viscose dominated propagation regimes, the dimension-

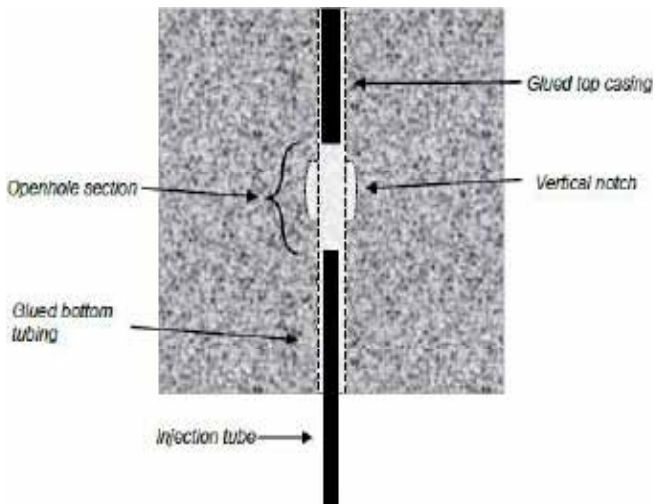


Figure 2. A schematic of a drilled hole with casing on top and an injection tube at the bottom. A notch is made in the open hole section to ease fracture initiation.

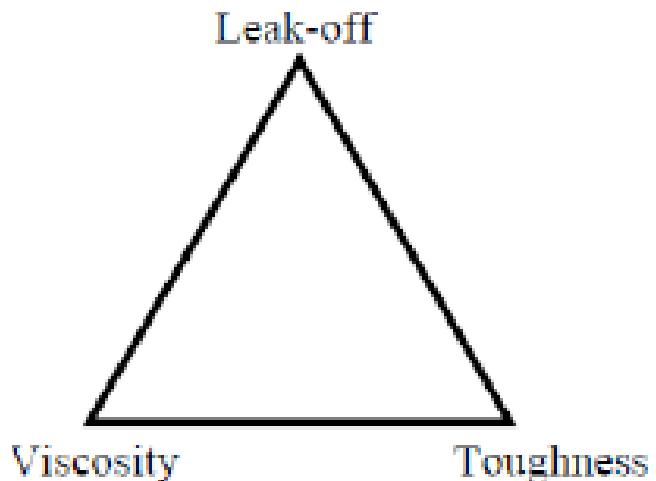


Figure 3. Triangular parametric space when only toughness, viscosity, and leak-off regimes are considered (simplified and reproduced from Bunger, 2005).

less toughness parameter of a Penny-Shaped fracture can be calculated as (Detournay, 2004):

$$\kappa = K' \left( \frac{t^2}{\mu^{15} Q^{13} E^{13}} \right)^{1/2} \quad (2)$$

In Equation 2,  $Q'$  is the flow rate and  $t$  is the experiment time. Other material properties are defined by Equation 3.

$$K' = \left( \frac{32}{\pi} \right)^{1/2} K_{IC}, \quad E' = \frac{E}{1-\nu^2}, \quad \mu' = 12\mu \quad (3)$$

Here,  $\mu$  is fracturing fluid viscosity,  $E$  is the rock Young's modulus, and  $\nu$  is Poisson's ratio. In Equation 2, the fracture propagation will be viscose dominated if  $\kappa$  is below one, whereas it is toughness dominated when the dimensionless toughness number exceeds four. In contrast with Equation 1, the dimensionless toughness parameter is time dependent; meaning the fracture regime may change from one type to another as time evolves. Also, the propagation regime was checked against another criterion proposed by Bungler (2005). In this method, the evaluation criterion is based on three characteristic times: leak-off, toughness, and viscosity.

## FRACTURING TEST INTERPRETATION

Figure 4 shows the pressure-time curves corresponding to both gauges before (inj2, gray solid line) and after (inj1) the chock; that is, wellbore pressure (after the chock, bold black) resulted from the scaled hydraulic-fracturing experiments of the 10 cm sample. The data was smoothed by using the moving average method in order to eliminate some parts of the recorded noise. The pressure drop between the pressure

transducer inj2 and the middle of the wellbore was neglected in these calculations. These two points are about 20–25 cm apart. From Figure 4 it is seen that a breakdown pressure of about 2,980 psi (20.5 MPa) was required to hydraulically fracture the sample (from transducer inj2, which is equivalent to wellbore pressure). This is the pressure needed to overcome both tensile strength of the rock and the induced hoop stresses.

Although the authors were able to monitor the slope of the wellbore pressure (pressurisation rate) curve during the course of the experiment, they were unable to distinguish the moment of fracture initiation; that is, the time at which the wellbore pressurisation rate was maximized. The reason is evidently shown in Figure 4 where the pressurisation rate curve does not indicate a clear maximum. Alternatively, the time at which the pressure difference between gauges inj1 and inj2 starts to increase from a constant value of 50 psi (or its derivative changes from zero to a positive value) may be taken as initiation pressure in the absence of aforementioned evidence. As shown in Figure 4, the initiation time is considered as the time the pressurisation curve, pressure difference between inj1 and inj2, and derivative of the pressure difference between inj1 and inj2 start to deviate from the plateau condition (straight line).

Some of these curves were not available during the time of the experiment and, therefore, a breakdown pressure at  $t=1,530$  s was used as the reference pressure. This resulted in some errors in the authors' calculations, which resulted in the induced fracture approaching the sample boundary; that is, the fracture was not contained from one side. The fracture, however, propagated along the maximum horizontal stress direction as expected. The difference between the initiation and breakdown pressure was about 167 s; this is longer than 100 s, which was the calculated time for fracture propagation and hence confirms why the fracture was not contained in the sample.

The fluid viscosity and injection rate should be modified based on the fact that they are functions of pressure. To sim-

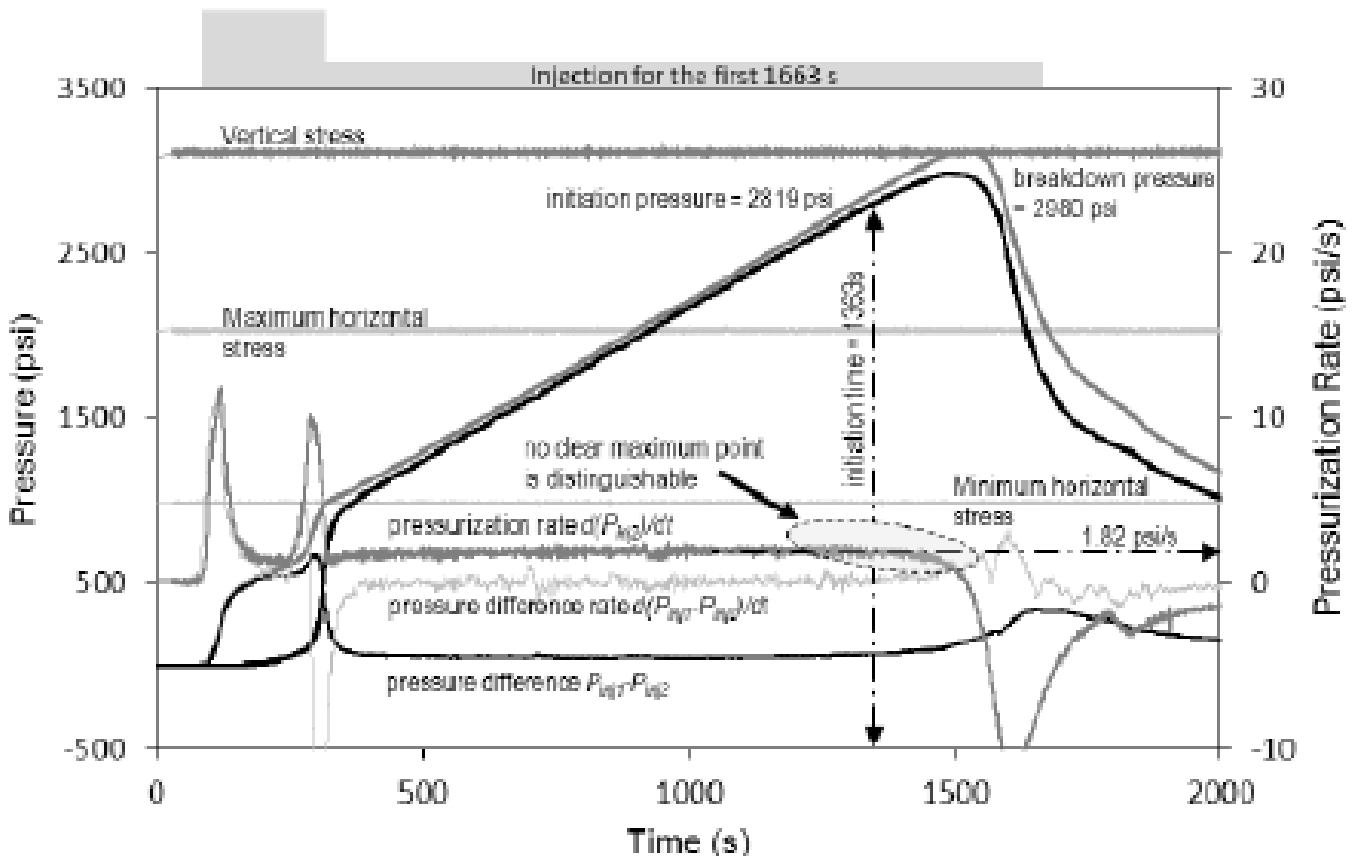


Figure 4. The pressure-time curve corresponding to hydraulic fracturing experiment of a 10 cm sample.

plify the problem, the pressure along the injection lines and the displacement chamber were considered to be the same as the wellbore pressure (i.e., reading at inj2). The actual injection rate and viscosity can be corrected for different pressures using Equations 4 and 5 (de Pater et al., 1994).

$$i_{corr} = i - p'(V_{sys} \cdot C_{sys}) \tag{4}$$

$$\mu_p = \mu_{nom} (1 + 6.5 \cdot 10^{-6} p) \tag{5}$$

In Equations 4 and 5,  $i_{corr}$  is the corrected injection rate,  $p'$  is the borehole pressurisation rate,  $V_{sys}$  is the total fluid volume of the system,  $C_{sys}$  is the system compressibility, and  $\mu_p$  is the corrected viscosity. Equation 5 shows the pressure (in psi) dependency of viscosity (cP). The constant value of this equation came from fracturing the fluid supplier. Figure 5 shows the plot of dimensionless pressure versus dimensionless time for the model, laboratory raw data, and the corrected data. The corrected data shows a better match with the model. The product of  $V_{sys} \cdot C_{sys}$  can be calculated as the flow rate and the average wellbore pressurisation rate (i.e., 1.82 psi/s) before the initiation (see Fig. 4).

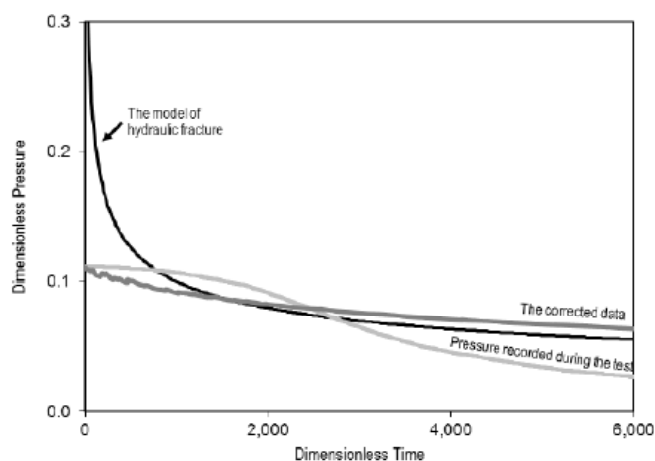


**Figure 5.** A comparison between the corrected dimensionless pressure from the experiment and the predicted pressure from the model.

## CONCLUSIONS

The first part of this paper presented the hydro-mechanical properties of the samples that should be measured for a fracturing laboratory test. The scaling laws, which are applied to simulate a field-scale fracture operation with lab scales, were introduced and their limitations and complexity discussed. The scaling laws were applied to design lab experiments performed using a true triaxial stress cell (TTSC), considering the effects of three independent stresses similar to field conditions. The results indicated the importance of sample heterogeneity in fracture propagation. Also, the results indicated the possibility of fracture twisting due to a change in the stress regime, which proves the concept that the induced fracture always propagates perpendicular to the direction of minimum principal stress.

## REFERENCES

- ADACHI, J., SIEBRITS, E., PEIRCE, A., AND DESROCHES, J., 2007—Computer simulation of hydraulic fractures. *International Journal of Rock Mechanics and Mining Sciences*, 44 (5), 739-757.
- ADACHI, J.I., 2001—Fluid-driven Fracture in Impermeable and Permeable Rock. PhD Dissertation. Minneapolis, Minnesota: University of Minnesota.
- ADACHI, J.I., AND DETOURNAY, E., 2007—Plane-strain propagation of a fluid-driven fracture. *Finite Toughness Self-similar Solution*. *International Journal of Fracture* 72, (4), 916-928.
- ATHAVALE, A.S., AND MISKIMINS, J.L., 2008—Laboratory Hydraulic Fracturing Tests on Small Homogeneous and Laminated Blocks. *The 42nd U.S. Rock Mechanics Symposium*, San Francisco, CA, June 29-July 2, 08-067.
- BUNGER, A., 2005—Near-surface Hydraulic Fracture. PhD Dissertation. Minneapolis: University of Minnesota.
- BUNGER, A., DETOURNAY, E. AND JEFFREY, R., 2005—Crack tip behavior in near-surface fluid-driven fracture experiments. *Comptes Rendus Mécanique*, 333 (4), 299-304.

*Continued next page.*

*Continued from previous page.*

- BUNGER, A., JEFFREY, R., AND DETOURNAY, E., 2005—Application of Scaling Laws to Laboratory-Scale Hydraulic Fractures. Alaska Rocks 2005, The 40th U.S. Symposium on Rock Mechanics, Anchorage, Alaska, June 25–29, 05–818.
- CHONG, K.P., KURUPPU, M.D., AND KUSZMAUL, J.S., 1987—fracture toughness determination of layered materials. Engineering Fracture Mechanics, 28 (1), 43–54.
- CLEARY, M.P., 1980—Comprehensive Design Formulae for Hydraulic Fracturing. Annual Fall Technical Conference and Exhibition of the Society of Petroleum Engineers of AIME, Dallas, Texas, September 21–24, 9259.
- DANESHY, A., 2004—Analysis of off-balance fracture extension and fall-off pressures. SPE International Symposium and Exhibition on Formation Damage Control. 18–20 February, Lafayette, Louisiana, 86471.
- DE PATER, C.J., CLEARY, M.P., QUINN, T.S., BARR, D.T., JOHNSON, D.E., AND WEIJERS, L., 1994—Experimental verification of dimensional analysis for hydraulic fracturing. SPE Production & Facilities, 9 (4), 230–238.
- DETOURNAY, E., 2004—Propagation regimes of fluid-driven fractures in impermeable rocks, International Journal of Geomechanics, 4 (1), 35–45.
- VAN DE KETTERIJ, R.G., 2001—Optimisation of the near-wellbore geometry of hydraulic fractures propagating from cased perforated completions. Dissertation. Amsterdam: Delft University Press.
- GARAGASH, D.I., 2006—Plane-strain propagation of a fluid fracture during injection and shut-in: Asymptotics of large toughness solutions. Engineering Fracture Mechanics, 73, 456–481.
- GARAGASH, D.I., DETOURNAY, E., 2005—Plane-strain Propagation of a Hydraulic Fracture: Small Toughness Solution. Journal of Applied Mechanics, 6,(72), 916–28.
- LHOMME, T., 2005—Initiation of hydraulic fractures in natural sandstones. PhD Dissertation. Delft, the Netherlands: Delft University of Technology.
- MACK, M.G., AND WARPINSKI, N.R., 2000—Mechanics of Hydraulic Fracturing. In: M. J. Economides and K. G. Nolte—Reservoir Stimulation (3rd edition). Chichester, England: John Wiley & Sons, LTD.
- MINDESS, S., YOUNG, J.F., AND DARWIN, D., 2002—Concrete (2nd Edition). New Jersey: Prentice Hall.
- MITCHELL, S.L., KUSKE, R., AND PEIRCE, A.P., 2007—An asymptotic framework for finite hydraulic fractures including leak-off. SIAM Journal of Applied Mathematics 2007, 67 (2), 364–386.
- EL RABAA, W., 1989—Experimental study of hydraulic fracture geometry initiated from horizontal wells. SPE Annual Technical Conference and Exhibition, San Antonio, Texas, 8–11 October, 19720-MS.
- SAVITSKI, A.A., AND DETOURNAY, E., 2002—Propagation of a penny-shaped, fluid-driven fracture in an impermeable rock: asymptotic solutions. International Journal of Solids Structure, 39 (26), 6311–6337.
- SCOTT, T.E., ZENG, Z.W., AND ROEGIERS, J.C., 2000—Acoustic emission imaging of induced asymmetrical hydraulic fractures. Proceedings of the Fourth North American Rock Mechanics Symposium, Seattle, Washington, July 3–August 3, 1129–1134.
- VONK, R.A., 1993— A micromechanical investigation of softening of concrete loaded in compression. Heron, 38 (3).
- WEIJERS, L., 1995—The near-wellbore geometry of hydraulic fractures initiated from horizontal and deviated wells. PhD Dissertation. The Netherlands: Delft University of Technology.

*Authors' biographies next page.*

## THE AUTHORS



**Mohammad Sarmadivaleh** is a post-doctoral fellowship in the Petroleum Engineering Department of Curtin University, working on a Co2 core flooding experiment. He completed his PhD at Curtin University in Perth as a result of a numerical and experimental study of the interaction of an induced hydraulic fracture with a natural interface. Mohammad holds a BSc in petroleum engineering (reservoir engineering), and an MSc in drilling and production engineering from Petroleum University of Technology (PUT), Iran, and an MEng in petroleum well engineering from Curtin University.

*mohammad.sarmadivaleh@curtin.edu.au*



**Amin Nabipour** is a PhD student in the Department of Petroleum Engineering at Curtin University. His present research focuses on numerical and experimental ultrasonic monitoring of fracture propagation. He received his BSc in mining engineering from Isfahan University of Technology (IUT) in 2006, with a thesis focused on the drilling bit performance

in horizontal drilling. In addition, he holds a Master of Petroleum Well Engineering Degree from Curtin University as well as in petroleum production and drilling engineering from Petroleum University of Technology (PUT), Tehran (2008) with a project on FEM modelling of stress induced in wellbore cement.

*amin.nabipour@postgrad.curtin.edu.au*



**Bahman Joodi** is a PhD candidate at Curtin University. After completing his Masters degree in petroleum well engineering from Curtin University in 2008, he worked as a well-site drilling engineer for two years. He is now working on a numerical and experimental simulation of drilling under bottom-hole conditions. Bahman holds a BSc in petroleum engineering, and an MSc in drilling and production engineering from Petroleum University of Technology (PUT), Iran, and an MEng in petroleum well engineering from Curtin University.

*bahman.joodi@postgrad.curtin.edu.au*



**Vamegh Rasouli** is an associate professor in the Department of Petroleum Engineering at Curtin University. He is a chartered professional engineer (CPEng), and is a registered engineer with the National Professional Engineers Register (NPER) of Australia. After completing his PhD in 2002 from Imperial College, London, Vamegh took up the position of assistant professor in the Department of Petroleum Engineering at Amirkabir University of Technology (Iran). In 2006, Vamegh joined the Department of Petroleum Engineering at Curtin University to add support to the delivery of the department's Master of Petroleum Well Engineering degree, and to carry out research in his specialist areas of wellbore stability, sanding, hydraulic fracturing, etc. He established the Curtin Petroleum Geomechanics Group (CPGG), which has completed a number of successful research and consulting projects. Vamegh has also been a consulting engineer on various geomechanics related projects with Schlumberger's Data and Consulting Services (DCS) in Perth.

*v.rasouli@curtin.edu.au*

